distinguish high grade glioma from low grade glioma. This may be useful in deciding the surgical strategy or selecting the site of stereotactic biopsy.

Acknowledgement

This work was supported in part by Grants-in-Aid for Advanced Medical Science Research by the Ministry of Education, Culture, Sports, Science, and Technology, Japan.

References

[1] Russell D, Rubinstein L. Tumours of central neuroepithelial origin. In: Rubinstein L, editor. Pathology of tumours of the nervous system. Baltimore: Williams & Wilkins; 1989. p. 83–350.
[2] Kayama T, Kumabe T, Tominaga T, Yoshimoto T. Prognostic value of complete response after the initial treatment for malignant astrocytoma. Neurol Res 1996;18:321–4.
[3] Black PM. Brain tumors. Part 1. N Engl J Med 1991;324:1471–6.
[4] Sugahara T, Korogi Y, Kochi M, Ikushima I, Shigematu Y, Hirai T, et al. Usefulness of diffusion-weighted MRI with echo-planar technique in the evaluation of cellularity in gliomas. J Magn Reson Imaging 1999;9:53–60.
[5] Burtscher IM, Stahlberg F, Holtas S. Proton (1H) MR spectroscopy for routine diagnostic evaluation of brain lesions. Acta Radiol 1997;38:953–60.
[6] Shimizu H, Kumabe T, Tominaga T, Kayama T, Hara K, Ono Y, et al. Noninvasive evaluation of malignancy of brain tumors with proton MR spectroscopy. AJNR Am J Neuroradiol 1996;17:737–47.
[7] Shimizu H, Kumabe T, Shirane R, Yoshimoto T. Correlation between choline level measured by proton MR spectroscopy and Ki-67 labeling index in gliomas. AJNR Am J Neuroradiol 2000;21:659–65.
[8] Shukla-Dave A, Gupta RK, Roy R, Husain N, Paul L, Venkatesh SK, et al. Prospective evaluation of in vivo proton MR spectroscopy in differentiation of similar appearing intracranial cystic lesions. Magn Reson Imaging 2001;19:103–10.
[9] Sfakianakis G. Preoperative grading of gangliogliomas using FDG PET and Tl-201 SPECT: comments from a nuclear medicine view. AJNR Am J Neuroradiol 1998;19:811.
[10] Kincaid PK, El-Saden SM, Park SH, Goy BW. Cerebral gangliogliomas: preoperative grading using FDG-PET and 201Tl-SPECT. AJNR Am J Neuroradiol 1998;19:801–6.
[11] Tamura M, Shibasaki T, Zama A, Kurihara H, Horikoshi S, Ono N, et al. Assessment of malignancy of glioma by positron emission tomography with 18F-fluorodeoxyglucose and single photon emission computed tomography with thallium-201 chloride. Neuroradiology 1998;40:210–5.
[12] Kallen K, Heiling M, Andersson AM, Brun A, Holtas S, Ryding E, et al. Evaluation of malignancy in ring enhancing brain lesions on CT by thallium-201 SPECT. J Neurol Neurosurg Psychiatry 1997;63:569–74.
[13] Kumabe T, Shimizu H, Sonoda Y, Shirane R. Thallium-201 single-photon emission computed tomographic and proton magnetic resonance spectroscopic characteristics of intracranial ganglioglioma: three technical case reports. Neurosurgery 1999;45:183–7.
[14] Pierpaoli C, Basser PJ. Toward a quantitative assessment of diffusion anisotropy. Magn Reson Med 1996;36:893–906.
[15] Basser PJ, Pierpaoli C. Microstructural and physiological features of tissues elucidated by quantitative-diffusion-tensor MRI. J Magn Reson B 1996;111:209–19.
[16] Bammer R, Augustin M, Strasser-Fuchs S, Seifert T, Kapeller P, Stollberger R, et al. Magnetic resonance diffusion tensor imaging for characterizing diffuse and focal white matter abnormalities in multiple sclerosis. Magn Reson Med 2000;44:583–91.
[17] Ciccarelli O, Werring DJ, Wheeler-Kingshott CA, Barker GJ, Parker GJ, Thompson AJ, et al. Investigation of MS normal-appearing brain using diffusion tensor MRI with clinical correlations. Neurology 2001;56:926–33.
[18] Ellis CM, Simmons A, Jones DK, Bland J, Dawson JM, Horsfield MA, et al. Diffusion tensor MRI assesses corticospinal tract damage in ALS. Neurology 1999;53:1051–8.
[19] Filippi M, Cercignani M, Inglese M, Horsfield MA, Comi G. Diffusion tensor magnetic resonance imaging in multiple sclerosis. Neurology 2001;56:304–11.
[20] Tievsky AL, Ptak T, Farkas J. Investigation of apparent diffusion coefficient and diffusion tensor anisotrophy in acute and chronic multiple sclerosis lesions. AJNR Am J Neuroradiol 1999;20:1491–9.
[21] Wieshmann UC, Clark CA, Symms MR, Franconi F, Barker GJ, Shorvon SD. Reduced anisotropy of water diffusion in structural cerebral abnormalities demonstrated with diffusion tensor imaging. Magn Reson Imaging 1999;17:1269–74.
[22] Daumas-Duport C, Scheithauer B, O'Fallon J, Kelly P. Grading of astrocytomas: a simple and reproducible method. Cancer 1988;62:2152–65.
[23] Kleihues P, Sobin LH. World Health Organization classification of tumors. Cancer 2000;88:2887.
[24] Jones DK, Lythgoe D, Horsfield MA, Simmons A, Williams SC, Markus HS, et al. Characterization of white matter damage in ischemic leukoaraiosis with diffusion tensor MRI. Stroke 1999;30:393–7.
[25] Hajnal JV, Doran M, Hall AS, Collins AG, Oatridge A, Pennock JM, et al. MR imaging of anisotropically restricted diffusion of water in the nervous system: technical, anatomic, and pathologic considerations. J Comput Assist Tomogr 1991;15:1–18.
[26] Le Bihan D. Anisotropic diffusion of brain whtie matter reviseted: restrictions, permeability and tortuosity. In: Book of abstracts. Presented at ISMRM, Berkeley, CA, 1996.
[27] Sinha S, Bastin ME, Whittle IR, Wardlaw JM. Diffusion tensor MR imaging of high-grade cerebral gliomas. AJNR Am J Neuroradiol 2002;23:520–7.
[28] Sevick RJ, Kanda F, Mintorovitch J, Arieff AI, Kucharczyk J, Tsuruda JS, et al. Cytotoxic brain edema: assessment with diffusion-weighted MR imaging. Radiology 1992;185:687–90.
[29] Anderson AW, Zhong J, Petroff OA, Szafer A, Ransom BR, Prichard JW, et al. Effects of osmotically driven cell volume changes on diffusion-weighted imaging of the rat optic nerve. Magn Reson Med 1996;35:162–7.
[30] Giannini C, Scheithauer BW, Weaver AL, Burger PC, Kros JM, Mork S, et al. Oligodendrogliomas: reproducibility and prognostic value of histologic diagnosis and grading. J Neuropathol Exp Neurol 2001;60:248–62.
[31] Sato Y, Ochiai H, Yamakawa Y, Nabeshima K, Asada Y, Hayashi T, et al. Brain surface ependymoma. Neuropathology 2000;20:315–8.
[32] Harada A, Fujii Y, Yoneoka Y, Takeuchi S, Tanaka R, Nakada T, et al. High-field magnetic resonance imaging in patients with moyamoya disease. J Neurosurg 2001;94:233–7.
[33] Fujii Y, Nakayama N, Nakada T. High-resolution T2-reversed magnetic resonance imaging on a high magnetic field system: technical note. J Neurosurg 1998;89:492–5.
[34] Shimony JS, McKinstry RC, Akbudak E, Aronovitz JA, Snyder AZ, Lori NF, et al. Quantitative diffusion-tensor anisotropy brain MR imaging: normative human data and anatomic analysis. Radiology 1999;212:770–84.
[35] Pierpaoli C, Jezzard P, Basser PJ, Barnett A, Di Chiro G. Diffusion tensor MR imaging of the human brain. Radiology 1996;201:637–48.

[36] Yoshiura T, Wu O, Zaheer A, Reese TG, Sorensen AG. Highly diffusion-sensitized MRI of brain: Dissociation of gray and white matter. Magn Reson Med 2001;45:734–40.
[37] Meyer JR, Gutierrez A, Mock B, Hebron D, Prager JM, Gorey MT, et al. High-*b*-value diffusion-weighted MR imaging of suspected brain infarction. AJNR Am J Neuroradiol 2000;21:1821–9.
[38] Melhem ER, Itoh R, Jones L, Barker PB. Diffusion tensor MR imaging of the brain: effect of diffusion weighting on trace and anisotropy measurements. AJNR Am J Neuroradiol 2000;21:1813–20.

ELSEVIER

Clinical Neurology and Neurosurgery xxx (2006) xxx–xxx

Clinical Neurology and Neurosurgery

www.elsevier.com/locate/clineuro

Alleviation of intracranial air using carbon dioxide gas during intraventricular tumor resection

Takaaki Beppu*, Kuniaki Ogasawara, Akira Ogawa

Department of Neurosurgery, Iwate Medical University, Morioka 020-8505, Japan

Received 30 July 2005; received in revised form 24 December 2005; accepted 3 January 2006

Abstract

Objectives/purposes: Postoperative vomiting occurs more frequently in patients after intraventricular surgery than after other intracranial surgeries. This has been attributed to intracranial air. Carbon dioxide gas (CO_2) has properties beneficial to the treatment of some medical disorders, displaying a higher specific gravity and more rapid absorption into surrounding tissues than air. We therefore, attempted to replace air with CO_2 during intra- and paraventricular tumor resections. The aim of the present study was to elucidate whether intracranial air after intraventricular surgery could be alleviated safely using CO_2, and investigate its clinical usefulness.

Patients and methods: CO_2 was introduced into the subdural space at 2 l/min through a silicon tube from time of dural incision to closure. Subjects comprised 40 patients alternately assigned to one of two groups: the trial group ($n=20$) receiving CO_2 treatment; and controls ($n=20$) without CO_2 treatment.

Results: Intra- and postoperatively, no patients showed complications caused by CO_2 treatment. Postoperatively, intraventricular gas shown on CT scans disappeared significantly sooner in the trial group than in controls. Frequency of postoperative vomiting was significantly lower in the trial group than in controls.

Conclusion: Intracranial air after intraventricular surgery can be safety alleviated using CO_2.

Keywords: Intraventricular surgery; Intracranial air; Carbon dioxide gas

1. Introduction

Intracranial air collection, or pneumocephalus, is a common occurrence after craniotomy, with asymptotic pneumocephalus reported at a frequency of 100% [1–4]. The amount of intracranial air may vary between individual patients postoperatively, and approximately 2–3 weeks is typically required for complete re-absorption [3]. Intracranial air rarely presents a clinical problem, but can potentially develop into tension pneumocephalus [4,5]. In particular, more cerebrospinal fluid (CSF) is drained during intraventricular surgery than during other intracranial surgeries, thereby creating more space for accumulation of intracranial air.

The specific gravity of carbon dioxide gas (CO_2) is higher than that of air at 1.54:1. In addition, CO_2 is more rapidly absorbed by surrounding brain tissues than air [6,7]. CO_2 is commonly used for insufflation of the pneumoperitoneum during laparoscopic surgery for three reasons: high solubility; combustion suppression properties; and lack of toxicity [8]. Postoperative vomiting occurs more frequently in patients after intraventricular surgery than after other intracranial surgeries and has been attributed to intracranial air [9]. In an attempt to alleviate intracranial air induced intraoperatively, we exploited the beneficial properties of CO_2 by replacing intracranial air with CO_2 during intraventricular surgery. The results are reported herein.

2. Patients and methods

2.1. Patients

The study protocol was approved by the Ethics Committee of Iwate Medical University. Patients recruited to this

* Corresponding author. Tel.: +81 196 51 5111x6603; fax: +81 196 25 8799.
E-mail address: tbeppu@iwate-med.ac.jp (T. Beppu).

0303-8467/$ – see front matter © 2006 Elsevier B.V. All rights reserved.
doi:10.1016/j.clineuro.2006.01.002

study were hospitalized in the Department of Neurosurgery at Iwate Medical University between January 1998 and June 2003. Entry criteria for this study comprised: (A) a diagnosis of intra- or paraventricular tumor based on the findings of preoperative computed tomography (CT) scans or magnetic resonance imaging (MRI); (B) a tumor bulk with a diameter >2 cm on CT or MRI; and (C) provision of written informed consent. Fourth ventricular tumors were limited to tumors originating from the cerebellum. Patients with tumor originating from the medulla oblongata were excluded from the present study. A total of 40 patients with newly diagnosed intra- or paraventricular tumors were subsequently enrolled into this study. Patients were assigned alternately to one of two study groups: the trial group, with CO_2 treatment; and the control group, without CO_2 treatment. The trial group comprised 20 patients (12 men, 8 women; mean age, 26.1; range, 1–71 years) with diagnoses of subependymoma in the lateral ventricle (LV) ($n=3$), astrocytoma in LV ($n=2$), central neurocytoma in LV ($n=1$), germinoma in the third ventricle (3rd V) ($n=4$), astrocytoma in the fourth ventricle (4th V) ($n=6$) and ependymoma in 4th V ($n=4$). The control group comprised 20 patients (10 men, 10 women; mean age, 20.3; range, 4–62 years) with subependymoma in LV ($n=2$), astrocytoma in LV ($n=3$), central neurocytoma in LV ($n=1$), germinoma in 3rd V ($n=4$), astrocytoma in 4th V ($n=6$), and ependymoma in 4th V ($n=4$). Obstructive hydrocephalus was present in 13 patients in the trial group (60%) and 12 patients in the control group (65%). Preoperative nausea and/or vomiting was identified in 11 trial group patients (55%) and 9 control group patients (45%).

2.2. Anesthesia and operation

Anesthesia was maintained using one of two methods: inhalation of 50% nitrous oxide gas (N_2O) with intravenous administration of sevoflurane (1–3%); or total intravenous anesthesia using propofol and fentanyl. Type of anesthesia was selected based on the needs of individual patients by anesthesiologists. N_2O was continuously supplied until skin closure. No patients underwent any drainage or shunt of CSF such as ventriculoperitoneal shunt prior to surgery or continuous spinal CSF drainage during surgery. All patients received osmotic diuretics to relax the cerebral cortex before dural incision. Temperature in the operating room was kept at 27 °C using an air conditioner. All patients underwent surgery in the supine or prone position only. Routine craniotomy was then performed according to suitable approaches for each tumor site.

2.3. Introduction of CO_2

For patients in the trial group, CO_2 was introduced into the surgical field using the techniques described by Kitakami et al. [6] with some modifications. Briefly, a sterile silicon tube connected to a CO_2 gas cylinder via an air filter was used to continuously introduce CO_2 at 2 l/min between the time of incision and closure of the dura into the intradural surgical field. The tip of the silicon tube was fixed at the edge of the incised dura in the surgical field using a silk string. The tube was positioned to avoid disturbance of the microscopic field (Fig. 1). $PaCO_2$ of arterial blood was recorded at 15-min intervals from the introduction of CO_2 until completion of surgery. Moreover, CSF of each patient was obtained from the surgical field immediately before dural closure, and pH of CSF was immediately measured.

Fig. 1. Surgical field in prone position for a patient with 4th ventricle tumor. The tip of silicon tube carrying CO_2 gas is fixed at the edge of incised dura. Arrow, tip of silicon tube; arrowhead, edge of incised dura.

For patients in the control group, operations were performed using standard techniques without introduction of CO_2. When suturing the dura, patients in both groups underwent flushing of the dural space using physiologal saline solution.

2.4. Statistical analysis

Several factors relating to intracranial condition were measured before surgery and then compared between groups: age; level of consciousness; tumor site; tumor size, presence of nausea and/or vomiting; and presence of obstructive hydrocephalus. Level of consciousness was estimated using the Glasgow Coma Scale (GCS). Tumor size was defined as the maximum diameter of tumor on CT or MRI. The Mann–Whitney *U*-test was used to evaluate differences in age, level of consciousness, and tumor size, while the chi-square test was used for tumor site. In addition, frequency of preoperative nausea and/or vomiting, anesthetic use of N_2O and frequency of hydrocephalus were compared between groups using Fisher's exact probability test. The values of $PaCO_2$ and pH of CSF were also compared between groups using Student's *t*-test.

Postoperatively, all patients underwent unenhanced CT immediately after surgery with sequential unenhanced CT performed every day until complete disappearance of the intracranial gaseous body. Mean duration until complete disappearance of intracranial gas collection on unenhanced CT was compared between groups using the Mann–Whitney *U*-test. Moreover, volume of intraventricular gaseous body was

Table 1
Comparisons of preoperative and intraoperative conditions between the trial group and the control group

	Trial group	Control group	p-value	Test
Age (mean ± S.D.)	26.1 ± 19.7	20.3 ± 18.0	0.26	MW
GCS (mean ± S.D.)	14.5 ± 1.1	14.2 ± 1.4	0.56	MW
Tumor site				
LV	6	6	0.92	CS
3rd V	4	5		
4th V	10	9		
Tumor size (cm)	3.4 ± 0.8	3.2 ± 0.8	0.37	MW
Presence of hydrocephalus	13	12	>0.99	FEP
Presence of nausea and/or vomiting before surgery	11	9		
Use of N_2O anesthesia	7	10	>0.99	FEP
$PaCO_2$ (mean ± S.D. mmHg)	34.6 ± 3.6	33.9 ± 3.2	0.78	ST
pHofCSF(mean ± S.D.)	7.5 ± 0.1	7.6 ± 0.2	0.16	ST

S.D.: standard deviation; GCS: Glasgow Coma Scale; LV: lateral ventricle; V: ventricle; MW: Mann–Whitney U-test; CS: chi-square test; FEP: Fisher's exact probability test; ST: Student's t-test.

measured for all patients using unenhanced CT immediately after surgery, calculated using the following simple formula [10]: intraventricular gaseous body volume (cm^3) = $ABC/2$, where A represents maximum diameter of gas accumulation and B represents maximum diameter perpendicular to A, on an axial slice showing maximal gas accumulation, and C represents the numbers of 1 cm thick CT slices on which the gaseous body is visualized. When more than two gaseous bodies were observed on CT, gas volume was determined as the sum of all gaseous bodies. Differences in gaseous body volume between groups were also analyzed using the Mann–Whitney U-test. Frequency of vomiting after surgery was compared between groups using Fisher's exact probability test. Period of vomiting incidence was also documented, and compared between groups using the Mann–Whitney U-test. For patients displaying postoperative vomiting, metoclopramide was administered intravenously as an anti-emetic two to three times per day until vomiting disappeared. Total cost for use of CO_2 and anti-emetics in each group was estimated. Values of $p < 0.05$ were considered statistically significant for all analyses. The same investigator (K.O.), who was blinded to subject grouping, visually assessed all CT findings and observed whether patients vomited within 24 h after surgery.

3. Results

No significant differences in patient characteristics or pre- or intraoperative findings were identified between trial and control groups (Table 1). No patients displayed any complications likely to be attributable to CO_2 during surgery. $PaCO_2$ and pH levels of CSF during surgery in the trial group were within the acceptable ranges of 25.0–35.0 mmHg (mean: 34.6 ± .3.6 mmHg) and 7.3–7.8 (mean: 7.5 ± .0.1), respectively. Neither value varied significantly from those in the control group.

The CT scans immediately after surgery revealed gaseous body collection filling the ventricles and subdural spaces in all patients in both groups (Fig. 2). Mean period required for complete disappearance of intracranial gaseous bodies was 2.3 ± 1.0 days in the trial group (range, 1–4 days) and 5.3 ± 1.6 days in the control group (range, 3–9 days), representing a significant difference between the 2 groups (Fig. 3). Intraventricular gaseous body volume immediately after surgery was 4.2 ± 2.5 cm^3 for the trial group and 6.7 ± 3.5 cm^3 for the control group, again representing a significant difference between groups (Fig. 4).

Vomiting occurred within 24 h after surgery for 5 of 20 patients in the trial group (25%) and 14 of 20 patients in the control group (70%). Frequency of postoperative vomiting was significantly lower in the trial group than in the control group ($p = 0.04$). The 5 patients presenting with postoperative vomiting in the trial group comprised 4 of 10 patients with 4th V tumor and 1 of 6 patients with LV tumor. Conversely, the 14 patients presenting with vomiting in the control group comprised all 9 patients with 4th V tumor, 3 of 5 patients with 3rd V tumor and 2 of 6 patients with LV tumor. Patients displaying vomiting after surgery were not the same patients who displayed vomiting before surgery. When limited to patients with 3rd V or LV tumor, numbers of patients presenting with vomiting after surgery tended to be smaller in the trial group than in the control group, although no significant differences were identified (Fisher's exact probability test; $p = 0.14$). The mean period of vomiting was 1.4 ± 0.5 days for the 5 patients in the trial group and 2.6 ± 1.2 days for the 14 patients in the control group, representing a significant difference between groups ($p = 0.02$). Mean daily cost for use of CO_2 and anti-emetics was 170 Japanese Yen (1.2 EUR) for the trial group and 620 Japanese Yen (4.4 EUR) for the control group. Costs were small and not significantly different between trial and control groups (Mann–Whitney U-test; $p = 0.052$).

4. Discussion

Several contributing factors associated with surgery have been recognized as readily introducing considerable amounts

Fig. 2. Representative unenhanced CT scan of a CO_2-treated patient immediately after surgery, showing accumulation of gas in ventricles and subdural spaces (A), and 1 day later showing complete disappearance of the gaseous body (B).

of air into the cranium [1,4,11–17]. Excluding trauma and infection not associated with surgery, these include: (A) N_2O anesthesia; (B) posterior fossa craniotomy in the sitting position; (C) intracranial surgery following CSF drainage; (D) use of osmotic diuretics during intracranial surgery; and (E) hydrocephalus. In the present study, anesthetic use of N_2O and the frequency of hydrocephalus did not differ significantly between the trial and control groups. In addition no patient underwent surgery in a sitting position or with CSF drainage, and all patients received osmotic diuretics intraoperatively. Furthermore, no significant differences in preoperative conditions (age, tumor site or tumor size) were found between groups. Pre-and intraoperative intracranial conditions were thus similar for patients in each group. This allowed for comparison of the follow-up CT and immediate postoperative vomiting between groups.

The CT obtained immediately after surgery showed that gaseous accumulation continued to fill the intracranium of patients treated with CO_2. This suggests that the collected gas would likely represent a mixture of CO_2 and air, as gas should be absorbed completely and almost immediately if the pictured gas represented 100% CO_2. However, sequential CT indicated that accumulated gas disappeared significantly sooner in the trial group than in the control group. Furthermore, gaseous body volume immediately after surgery was significantly smaller in the trial group than in the control group. This suggests more rapid absorption of the gaseous body in the trial group than in the control group, immediately after surgery. Higher patient body temperature than operating room temperature may have caused expansion of

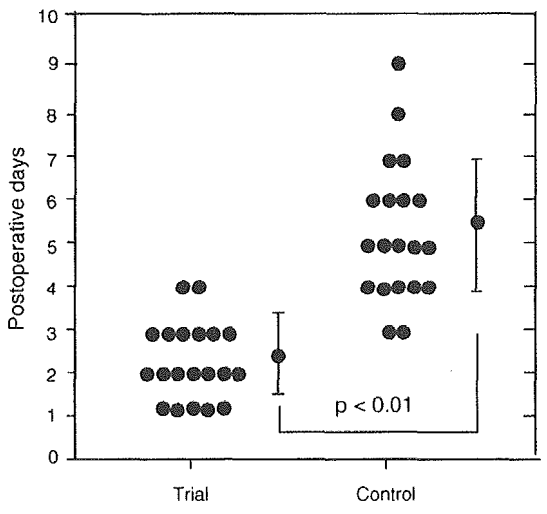

Fig. 3. Postoperative period for complete disappearance of gas on postoperative CT scans for trial (CO_2) and control (air) groups.

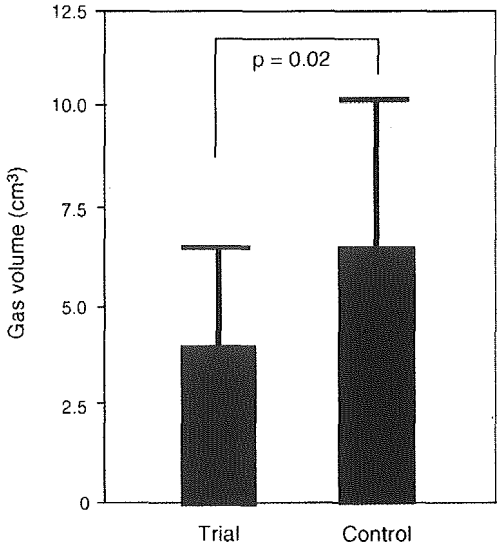

Fig. 4. Volume of intraventricular gas measured by CT immediately after surgery for trial (CO_2) and control (air) groups.

the intracranial gaseous body. However, temperatures were the same for patients in both groups, which indicate that the rapid alleviation of gaseous volume in the trial group was due to properties of the CO_2 gas itself. No patients showed any complications likely to be attributable to CO_2 during and after surgery. $PaCO_2$ levels and pH levels of CSF during surgery in patients treated with CO_2 were within acceptable levels, and did not differ significantly from levels in the control group. We believe that intracranial air after intraventricular surgery can be safety alleviated using CO_2.

Examination of postoperative symptoms in this study was limited to the presence or absence of vomiting, as other symptoms such as vital signs, recovery of consciousness; cranial nerve palsy or transient hemiparesis of the extremities are greatly influenced by anesthetic technique and type of surgical procedure. Subjective symptoms such as headache and nausea without vomiting were also not examined, because estimation of these symptoms was difficult under the unstable level of consciousness displayed by patients during first 24 h after surgery. In the present study, frequency of postoperative vomiting was significantly lower for the trial group than for the control group. Rapid absorption of CO_2 gas and the small volume of gas accumulation in the trial group may have prevented postoperative vomiting. At time of the study, vomiting was a common complication in pneumoencephalography, in addition to headaches, changes in pulse and body temperature [18,19]. An earlier study suggested that air entering the 4th V produces irritation of the medullary centers [19]. Recent studies have suggested that the essential region for coordinating vomiting is located in the brainstem between the levels of the obex and the retrofacial nucleus [20–24]. The area postrema is one vomiting sensor on the dorsal surface of the medulla oblongata, and is positioned to detect emetic agents in both blood and CSF, due to the lack of a blood–brain barrier [21]. In the present study, alleviation of intraventricular air using CO_2 might have mitigated direct irritation of the vomiting coordinating circuitry on the dorsal surface of the medulla oblongata in patients with 4th V tumor. Although no significant differences were noted between groups, use of CO_2 tended to be associated with decreased frequency of vomiting in patient with supratentorial intraventricular tumor in the trial group. Neurosurgeons frequently encounter postoperative vomiting in patients undergoing supratentorial intraventricular surgery. The mechanisms underlying postoperative vomiting after supratentorial intraventricular surgery remain unclear [9]. Fujimura et al. [25] reported that malignant astrocytoma patients with dissemination to CSF display intractable vomiting, but MRI could not detect any lesion on vomiting centers of the medulla oblongata. In that report, a small population of tumor cells was considered likely to have contributed to biological stimulation of the vomiting center. The vomiting coordinating circuitry on the dorsal surface of the medulla oblongata might perceive changes in pressure and biological characters of CSF. Use of CO_2 rapidly alleviates intraventricular air accumulation in patients with supratentorial intraventricular tumor, thus mitigating stimulation to the vomiting-coordinating circuitry on the dorsal surface of the medulla oblongata. Patients who display vomiting immediately after surgery are in danger of aspiration pneumonia. The present technique may contribute to decreased postoperative vomiting in patients undergoing intraventricular surgery. Furthermore, the cost for use of CO_2 is as low or lower than the cost for use of anti-emetics.

Numerous techniques have been used to prevent accumulation of intracranial air including flushing a physiological saline solution into the surgical field [26], alteration of anesthetic technique [14], and temporarily blockage of CSF drainage during surgery [4]. The present technique, although still in the trial stages, does appear to safety alleviate intracranial air with CO_2, as no patients showed obvious complications during surgery.

Given these findings, our technique may offer a method for alleviating intracranial air after intraventricular surgery.

Acknowledgement

This work was supported by the Advanced Medical Science Center at Iwate Medical University.

References

[1] Domino KB, Hemstad JR, Lam AM, Laohaprasit V, Mayberg TA, Harrison SD, et al. Effect of nitrous oxide on intracranial pressure after cranial-dural closure in patients undergoing craniotomy. Anesthesiology 1992;77:421–5.
[2] Harders A, Gilsbach J, Weigel K. Supratentorial space occupying lesions following infratentorial surgery: early diagnosis and treatment. Acta Neurochir (Wien) 1985;74:57–60.
[3] Reasoner DK, Todd MM, Scamman FL, Warner DS. The incidence of pneumocephalus after supratentorial craniotomy. Observations on the disappearance of intracranial air. Anesthesiology 1994;80:1008–12.
[4] Satapathy GC, Dash HH. Tension pneumocephalus after neurosurgery in the supine position. Br J Anaesth 2000;84:115–7.
[5] Lunsford LD, Maroon JC, Sheptak PE, Albin MS. Subdural tension pneumocephalus. J Neurosurg 1979;50:525–7.
[6] Kitakami A, Ogawa A, Hakozaki S, Kidoguchi J, Obonai C, Kubo N. Carbon dioxide gas replacement of chronic subdural hematoma using single burr-hole irrigation. Surg Neurol 1995;43:574–81.
[7] Liberson F. The use of various gases in encephalography: summary of 210 cases, using simultaneous displacement apparatus. Am J Med Sci 1933;185:478.
[8] Diemunsch PA, Torp KD, Van Dorsselaer T, Mutter D, Diemunsch AM, Schaeffer R, et al. Nitrous oxide fraction in the carbon dioxide pneumoperitoneum during laparoscopy under general inhaled anesthesia in pigs. Anesth Analg 2000;90:951–3.
[9] DeAngelis LM, Gutin PH, Leibel SA, Posner JB. Intracranial tumors. Diagnosis and treatment. London: Martin Dunitz Ltd.; 2002. p. 73.
[10] Broderick JP, Brott TG, Grotta JC. Intracranial hemorrhage volume measurement. Stroke 1994;25:1081.
[11] Artru AA. Nitrous oxide plays a direct role in the development of tension pneumocephalus intraoperatively. Anesthesiol 1982;57:59–61.
[12] Friedman GA, Norfleet EA, Bedford RF. Discontinuance of nitrous oxide does not prevent tension pneumocephalus. Anesth Analg 1981;60:57–8.

[13] Ram Z, Knoller N, Findler G, Sahar A. Delayed intraventricular tension pneumocephalus complicating posterior fossa surgery for cerebellar medulloblastoma. Childs Nerv Syst 1992;8:351–3.
[14] Saxena S, Ambesh SP, Saxena HN, Kumar R. Pneumocephalus and convulsions after ventriculoscopy: a potentially catastrophic complication. J Neurosurg Anesthesiol 1999;11:200–2.
[15] Toung T, Donham RT, Lehner A, Alano J, Campbell J. Tension pneumocephalus after posterior fossa craniotomy: report of four additional cases and review of postoperative pneumocephalus. Neurosurgery 1983;12:164–8.
[16] Tripathy P, Chowdhury BK, Bhattacharya A, Munshi AK, Bhattacharya MK. Tension pneumocephalus following posterior cranial fossa surgery in sitting position. J Indian Med Assoc 1995;93: 109–10.
[17] Di Lorenzo N, Caruso R, Floris R, Guerrisi V, Bozzao L, Fortuna A. Pneumocephalus and tension pneumocephalus after posterior fossa surgery in the sitting position: a prospective study. Acta Neurochir (Wien) 1986;83:112–5.
[18] Bergeron RT, Rumbaugh CL. Problems incident to pneumographic and other nonangiographic radiologic contrast studies of the brain. Bull Los Angeles Neurol Soc 1971;36:1–10.
[19] Taveras JM, Wood EH. Intracranial pneumography. In: Taveras JM, Wood EH, editors. Diagnostic neuroradiology. Baltimore: Williams and Williams; 1964. p. 1248–9.
[20] Borison HL. Area postrema: chemoreceptor circumventricular organ of the medulla oblongata. Prog Neurobiol 1989;32:351–90.
[21] Hornby PJ. Central neurocircuitry associated with emesis. Am J Med 2001;111:106S–12S.
[22] Koga T, Qu R, Fukuda H. The central pattern generator for vomiting may exist in the reticular area dorsomedial to the retrofacial nucleus in dogs. Exp Brain Res 1998;118(2):139–47.
[23] Millar AD. Central mechanisms of vomiting. Dig Dis Sci 1999;44: 39–43.
[24] Millar AD, Leslie RA. The area postrema and vomiting. Front Neuroendocrinol 1994;15:301–20.
[25] Fujimura M, Kumabe T, Jokura H, Shirane R, Yoshimoto T, Tominaga T. Intractable vomiting as an early clinical symptom of cerebrospinal fluid seeding to the fourth ventricle in patients with high-grade astrocytoma. J Neuro-Oncol 2004;66:209–16.
[26] Toung T, Donham RT, Campbell JN. Prevention of tension pneumocephalus. Anesthesiology 1982;57:65–6 (letter).

Int. J. Cancer: **117**, 41–50 (2005)

Downregulation of laminin α4 chain expression inhibits glioma invasion *in vitro* and *in vivo*

Shigeyuki Nagato[1]*, Kou Nakagawa[1], Hironobu Harada[1], Shohei Kohno[1], Hironobu Fujiwara[2], Kiyotoshi Sekiguchi[2], Shiro Ohue[1], Shinji Iwata[1] and Takanori Ohnishi[1]
[1]*Department of Neurosurgery, Ehime University School of Medicine, Ehime, Japan*
[2]*Institute for Protein Research, Osaka University, Osaka, Japan*

The laminin family is a structural constituent of the extracellular matrix that plays an essential role in promoting the motility of infiltrative tumor cells. We investigated the role of laminin α4 chain, a subset of laminin-8, -9 and -14, in the motile and invasive activities of human glioma cells. All malignant glioma cell lines examined expressed more mRNA for the laminin α4 and β1 chains than for the β2 chain, indicating that these cells predominantly express the laminin-8 isoform. Introducing an antisense oligonucleotide for laminin α4 chain (AS-Ln-α4) into the glioma cells resulted in downregulation of laminin α4 expression. AS-Ln-α4 also significantly suppressed glioma cell adhesion and migration. Furthermore, invasiveness was significantly reduced in cells transfected with AS-Ln-α4 compared to those transfected with the sense oligonucleotide (S-Ln-α4). Indeed, when glioma spheroids were implanted into rat brain slices, AS-Ln-α4-transfected cells failed to invade surrounding normal brain tissues. In addition, intracerebral injection of glioma cells transfected with AS-Ln-α4 into nude mice resulted in the formation of a noninvasive tumor, whereas injection of cells transfected with S-Ln-α4 resulted in diffuse invasion of brain tissue. These results suggest that mainly laminin-8 is essential for the invasive activity of human glioma cells; thus, a novel therapeutic strategy could target this molecule to treat patients with malignant glioma.

Key words: glioma; invasion; laminin; antisense

Almost all primary brain tumors of glial cell origin, especially malignant gliomas, are characterized by high invasiveness. This invasive property of gliomas usually prevents complete remission as infiltrative growth into the surrounding normal brain is responsible for the ineffectiveness of traditional therapeutic modalities. Various therapeutic protocols, including radiotherapy and chemotherapy, have been attempted to treat malignant gliomas; but the overall prognosis remains poor, with median survival of about 1 year.[1] The failure of glioma therapy results from resistance of invading cells to irradiation and anticancer drugs and leads to tumor recurrence. Therefore, an essential problem presented by gliomas is the tendency of malignant cells to diffusely invade the adjacent normal brain tissue. To establish an effective strategy to overcome glioma invasion, the molecular and cellular mechanisms of tumor invasion must be understood in detail. However, the molecular features underlying malignant glioma invasion remain obscure. Cell motility with local degradation of the ECM is essential for tumor cell invasion. The ECM can be defined as a complex mixture of proteins, proteoglycans and adhesive glycoproteins that provides structural and mechanical support to cells and tissues.[2] However, the structural and regulatory proteins of the ECM function cooperatively to regulate a variety of cellular processes, including cell migration and adhesion. Therefore, the biologic interactions between ECM components and glioma cells should be clarified to elucidate the mechanism of glioma invasion.

Expression of ECM proteins such as fibronectin, laminin and various types of collagen has been augmented both *in vitro* and *in vivo* in human malignant gliomas compared to benign brain tumors.[3–8] Laminins, as heterotrimeric glycoproteins comprising α, β and γ chains, are biologically active in neoplastic tissues and promote cell motility and growth, angiogenesis and metastasis.[9–13] To date, 5 α, 3 β and 3 γ chains have been identified; and combinations of these chains constitute 15 distinct laminin isoforms.[9,12,13] Since cellular responses to the various laminin isoforms are cell- and tissue-specific, laminin expression is dependent on the type of neoplasm.[9,12] Ljubimova *et al.*[14] reported that among the many genes overexpressed in various glial tumors and tissues adjacent to malignant gliomas, the laminin α4 chain is specifically upregulated compared to normal brain tissue. They also confirmed that laminin α4 chain mRNA is significantly increased in high-grade gliomas compared to low-grade gliomas and normal brain tissue.[15] Moreover, upregulated laminins containing an α4 chain play important roles in the development of angiogenesis and tumor progression in human glial tumors.[16] However, little is known about the relationship between α4 chain–containing laminins (laminin-8, -9 or -14) and glioma cell invasion. In the present study, we examined the biologic significance of laminins containing an α4 chain with respect to human glioma cell migration and invasion. The results showed that downregulation of laminin α4 chain expression decreased tumor cell motility and invasion *in vitro* and *in vivo*. Targeting the laminin α4 chain might have novel potential as an antiinvasive therapy for patients with malignant gliomas.

Material and methods

Cell lines and cell culture

Human malignant glioma cell lines U251 and U373 were generously provided by Dr. N. Arita (Hyogo College of Medicine, Hyogo, Japan); T98G was obtained from the HSRRB; and LN18 was generously donated by Dr. M. Tada (Hokkaido University School of Medicine, Sapporo, Japan). Human adenocarcinoma cell line HSG was obtained from the HSRRB (Osaka, Japan). All cell lines were maintained in DMEM with 10% heat-inactivated FBS containing 100 units/ml penicillin, 100 μg/ml streptomycin and 0.25 μg/ml amphotericin (GIBCO, Grand Island, NY) and incubated at 37°C under standard conditions of 100% humidity, 95% air and 5% CO_2.

Abbreviations: AS-Ln-α4, antisense laminin α4 chain; ECM, extracellular matrix; EPEI, ethoxylated polyethylenimine; GAPDH, glyceraldehyde-3-phosphate dehydrogenase; H&E, hematoxylin and eosin; HEPES, 4-(2-hydroxyethyl)-1-piperazine ethanesulfonic acid; HSRRB, Health Science Research Resources Bank; MAb, monoclonal antibody; MMP-2, matrix metalloproteinase-2; PVDF, polyvinylidene difluoride; S-Ln-α4, sense laminin α4 chain.

Grant sponsor: Integrated Center of Sciences, Ehime University; Grant sponsor: Ministry of Education, Culture, Sports, Science and Technology, Japan; Grant number: 14571314.

***Correspondence to:** Department of Neurosurgery, Ehime University School of Medicine, Shitsukawa, Shigenobu-cho, Onsen-gun, Ehime 791-0295, Japan. Fax: +81-89-960-5340. E-mail: nagato@m.ehime-u.ac.jp

Received 25 August 2004; Accepted after revision 31 January 2005
DOI 10.1002/ijc.21102
Published online 24 May 2005 in Wiley InterScience (www.interscience.wiley.com).

RT-PCR

Total RNA extracted from 4 human malignant glioma cell lines using acid guanidinium isothiocyanate phenol chloroform was used as the template for cDNA synthesis.[17] Human laminin α4, β1and β2 chains were analyzed by RT-PCR using the following primer pairs: laminin α4 chain forward 5′-CTCCATCTCACTG-GAT AATGGTACTG-3′ and reverse 5′-GACACTCATAAAGA-GAAGTGTGGACC-3′,[14] laminin β1 chain forward 5′-TTGGAC-CAAGATGTCCTGAG-3′ and reverse 5′-CAATATATTCTG-CCTCCCCG-3′[18] and laminin β2 chain forward 5′-CACTGTG AGCTCTGTCGGCCCTTC-3′ and reverse 5′-CAAGGAGTGCT-CCCAGGCACTGTG-3′.[19] Each cycle consisted of 30 sec of denaturation at 94°C, 60 sec of annealing at 60°C and 60 sec of elongation at 72°C, with 32 cycles performed.[14] GAPDH was used as the endogenous control. RT-PCR products were analyzed by electrophoresis on 2% agarose gels.

Antisense oligonucleotides

Gene Tools (Eugene, OR) custom-designed the morpholino oligonucleotide (M-oligo) of laminin α4 chain using the α4 antisense 5′-AGCTCAAAGCCATTTCTCCGCTGAC-3′ (EMBL accession number for laminin α4 gene X91171) and the α4 sense 5′-GTCAGCGGAGAAATGGCTTTGAGCT-3′ sequences with the 2-component special delivery protocol. One component is a paired duplex of M-oligo and a partially complementary DNA oligo (morpholino/DNA). The other is the weakly basic delivery reagent EPEI. Morpholino/DNA (0.5 mM) was incubated with EPEI at room temperature for 20 min. Glioma cells were cultured with the morpholino/DNA/EPEI mixture in a CO_2 incubator for 3 hr, and then the mixture was replaced with fresh medium containing serum. Glioma cells could be assayed from 16 hr thereafter. The medium was aspirated and replaced with medium without serum every 2 days, and the inhibitory effect of M-oligo was assessed at 3, 5 and 7 days.

Western blots

Serum-free conditioned medium (5 ml/10 cm culture dish) containing S-Ln-α4 or AS-Ln-α4 oligonucleotide or neither was concentrated by ammonium sulfate precipitation. Protein (10 μg) from each sample was resolved by 6% SDS-TRIS glycine gel electrophoresis and transferred to a PVDF membrane (Bio-Rad, Hercules, CA). Membranes were incubated with a primary MAb against laminin α4 chain (clone 2-11H; provided by Drs. K. Sekiguchi and H. Fujiwara, Institute for Protein Research, Osaka University, Osaka, Japan) or laminin β1 chain (Santa Cruz Biotechnology, Santa Cruz, CA), followed by horseradish peroxidase–conjugated sheep antimouse IgG antibody (Amersham, Piscataway, NJ). Band intensities were determined using NIH image analysis software (National Institutes of Health, Bethesda, MD), and the ratio to laminin β1 chain was determined.

Cell viability assay

Three days after treatment with S-Ln-α4 or AS-Ln-α4, 3-4, 5-dimethylthiazol-2,5-diphenyltetrazolium bromide was added to each well of a 6-well plate. Cells were trypsinized and viable cells assessed by trypan blue exclusion.[20] Glioma cell viability was compared with that of cells without any treatment.

Adhesion assay

Cell adhesion assays were performed as described.[21] Briefly, 4×10^4 glioma cells/well in 96-well culture plates cells were incubated for 24 hr at 37°C in serum-free conditioned medium with AS-Ln-α4 or S-Ln-α4. Plates were washed with PBS to remove unattached cells; then, attached cells were fixed with 3.7% formaldehyde and stained using toluidine blue (Sigma, St. Louis, MO). Thereafter, cells were washed with PBS and dissolved in 100 μl of 1% SDS. Absorbance was measured at 620 nm using a microplate reader (ImmunoMini NJ-2300; System Instrument, Chiba, Japan).

Migration assay

Migratory responses of glioma cells to their own conditioned medium were assessed using the modified Boyden method with 48-well microchemotaxis chambers (Nucleopore, Pleasanton, CA) as described.[22,23] In brief, glioma cells transfected with AS-Ln-α4 or S-Ln-α4 were harvested and resuspended in DMEM containing 0.1% BSA at a density of 8×10^5/ml. Cell suspensions (30 μl) were placed in the upper well of the chamber, and serum-free conditioned medium was placed in the lower well as a chemoattractant. The filter was a polyvinylpyrrolidone-free polycarbonate membrane with 8.0 μm pores (Millipore, Bedford, MA). The chamber was incubated for 4 hr at 37°C under the standard conditions described above, and cells that had migrated to the lower surface of the filter were fixed and stained with Diff-Quik (Scientific Products, Harleco, Gibbstown, NJ). Cells were counted in 4 independent fields (0.25 mm^2/well).

Invasion assay

The invasive activity of glioma cells was assayed *in vitro* using Falcon cell culture inserts and a reconstituted basement membrane, collagen type IV (both from Becton Dickinson, Bedford,

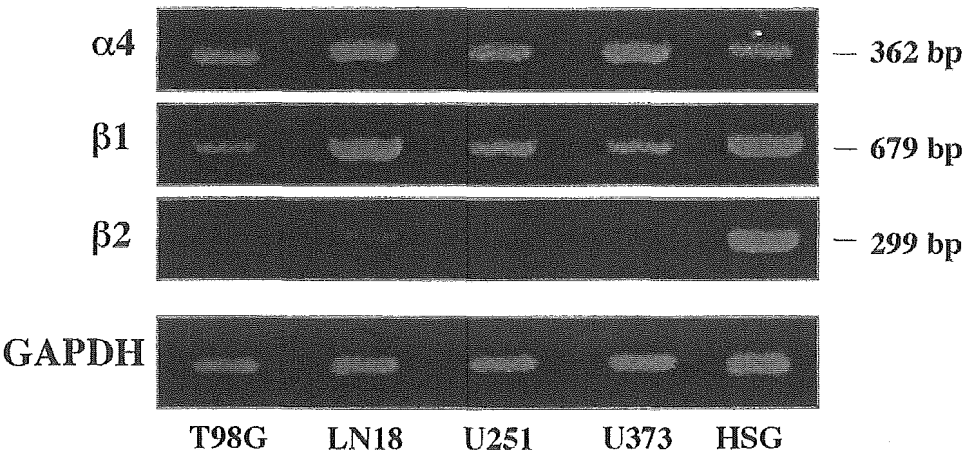

FIGURE 1 – Expression of laminin α4, β1 and β2 chain mRNA in human glioma cell lines T98G, LN18, U251 and U373. Total RNA extracted from glioma cells was amplified by RT-PCR to obtain transcripts of α4 (362 bp), β1 (679 bp) and β2 (299 bp) chains. Products of PCR resolved by electrophoresis on 2% agarose gels were visualized by ethidium bromide staining. Expression of laminin α4, β1 and β2 chains in human adenocarcinoma cell line (HSG) was used as a positive control. GAPDH was the internal control.

MA), as described.[24–27] Briefly, glioma cells treated with AS-Ln-α4 or S-Ln-α4 in DMEM containing 0.1% BSA were seeded onto the upper sides of insert filters coated with collagen IV (60 μg/insert) gel at a density of 1×10^5/insert. The lower compartments of the Falcon 24-well plates contained 500 μl of conditioned medium as a chemoattractant. After 1, 2 or 3 days at 37°C under the standard conditions, the lower surfaces of culture inserts were fixed and stained with Diff-Quik. Invasive activities were quantified as described for migration assays.

Invasion assay in brain slice model

All animal experiments were conducted in accordance with the guidelines for animal experiments of the Ehime University Committee for Ethics of Animal Experimentation.

Brain slice cultures were obtained by modifying the Stoppini method[28] as described.[29,30] Briefly, whole brains were removed from 2-day-old neonatal male Wistar rats (Kurea, Kagawa, Japan) under sterile conditions and placed in HBSS (Sigma). Brains were mounted on the stage of a microslicer (Dosaka, Kyoto, Japan) and cut into 500 μm coronal slices, which were transferred onto 30 μm Millicell-CM inserts with 0.4 μm pores (Millipore) in 6-well culture plates. Wells contained 1.0 ml of 50% EMEM (Sigma) with HEPES (Sigma), 25% HBSS, 25% heat-inactivated horse serum and 6.5 mg/ml glucose. Brain slices were incubated at 37°C in a humidified atmosphere of 95% air and 5% CO_2, and the culture medium was replaced with fresh medium twice each week.

Glioma cells transfected with AS-Ln-α4 or S-Ln-α4 were fluorescently labeled with PKH26 (rhodamine) using a kit (Zynaxis, Cell Science, Malvern, PA) as described.[31] In brief, 1.0×10^7 harvested glioma cells in serum-free DMEM were resuspended in 1 ml of diluent C, and then PKH26 dye in 1 ml of diluent C (2×10^{-6} M) was added. After incubating the cells at room temperature for 4 min, the labeling reaction was stopped by adding 2 ml of FBS. After adding 4 ml of DMEM containing 10% FBS, free PKH26 dye was removed by thoroughly washing the cells.

Rhodamine-labeled glioma cells (5×10^6) seeded into 1.25% agar-coated 10 cm culture dishes were continuously agitated on an XR-36 mixer (Taitec, Saitama, Japan) at 37°C under the standard conditions to form 300–400 μm spheroids. One rhodamine-labeled glioma cell spheroid was put on a rat brain slice and cocultured at 37°C under the standard conditions for 3 days. Cell invasion was observed by fluorescence microscopy on days 0 and 3.

U373 glioma transplantation model

Nude mice (6–8 weeks old) anesthetized with 0.9 mg/kg of pentobarbital sodium (Sigma) were held in a stereotactic frame. A midline skin incision was made in the head, and a burr hole was drilled in the skull 1 mm anterior to the coronal suture and 1.5 mm lateral to the midline to expose the dura. Rhodamine-labeled U373 human glioma cells (5×10^4) treated with AS-Ln-α4 or S-Ln-α4 in 3 μl of PBS were injected to a depth of 3 mm from the dura mater using a Hamilton (Reno, NV) syringe connected to the stereotactic frame. The needle was retained for 2 min and slowly withdrawn over a 2 min period.

Three days after tumor transplantation, rats were decapitated. The whole brain was removed, plunged into isopentane at –80°C and cut into frozen blocks, which were further sectioned into 20 μm coronal slices. The invasive activity of rhodamine-labeled U373 glioma cells in coronal sections was observed under a fluorescence microscope and then histologically assessed by staining with H&E.

Statistics

Results are representative of experiments repeated at least 3 times, and values are expressed as means ± SD. Statistical comparisons between groups were carried out using Student's *t*-test (StatView; SAS Institute, Cary, NC). $p < 0.05$ was considered statistically significant.

Results

Expression of laminin α4, β1 and β2 chain mRNA in human glioma cells

Laminin α4 chain is a constituent of laminins-8 (α4β1γ1), -9 (α4β2γ1) and -14 (α4β2γ3). To assess the expression profiles of laminins containing the α4 chain in human glioma cell lines, we initially investigated the mRNA levels of the laminin α4, β1 and β2 chains. Figure 1 shows the constitutional mRNA expression of these laminin chains, as determined by RT-PCR. We detected laminin α4 and β1 chain mRNA in all cell lines. However, lami-

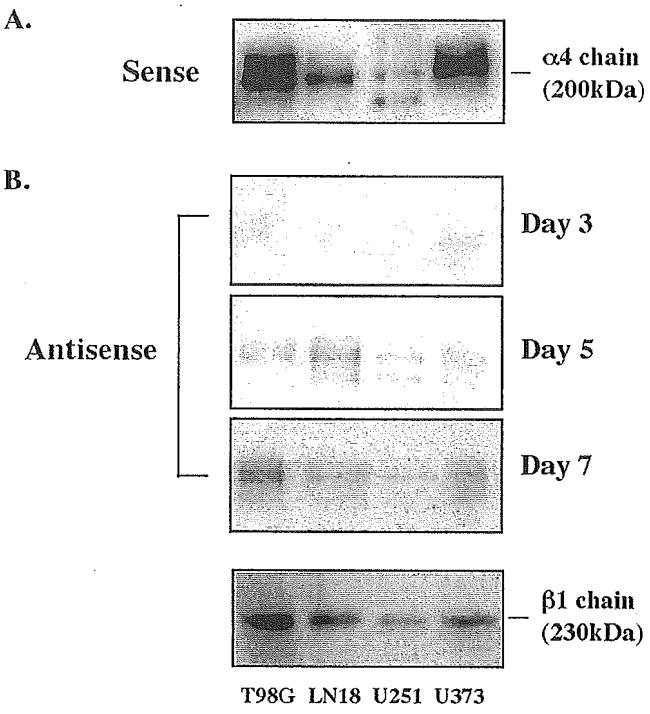

FIGURE 2 – Effects of AS-Ln-α4 on the protein expression of laminin α4 chain. Total proteins were obtained from serum-free culture medium from glioma cells treated with S-Ln-α4 or AS-Ln-α4. Equal amounts of protein from each treatment group were subjected to Western blotting using antilaminin α4 chain antibody. *(a)* Expression of laminin α4 chain in 4 glioma cell lines incubated with S-Ln-α4 for 3 days. *(b)* Effects of AS-Ln-α4 on expression of laminin α4 chain at 3, 5 and 7 days. Expression of laminin β1 chain was used as an internal control. *(c)* Columns represent densitometric quantification of α4 chain band from each time point of cells treated with AS-Ln-α4 in each cell line. Ratios of laminin α4 chain to β1 chain are presented as means ± SD of 3 independent experiments.

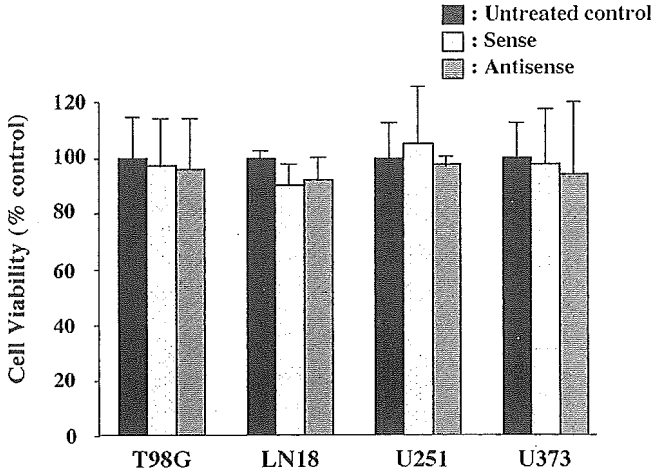

FIGURE 3 – Cell viability after treatment with sense or antisense oligonucleotides was assessed using trypan blue exclusion in each glioma cell line. Values shown as means ± SD were percentages for the viability of untreated cells.

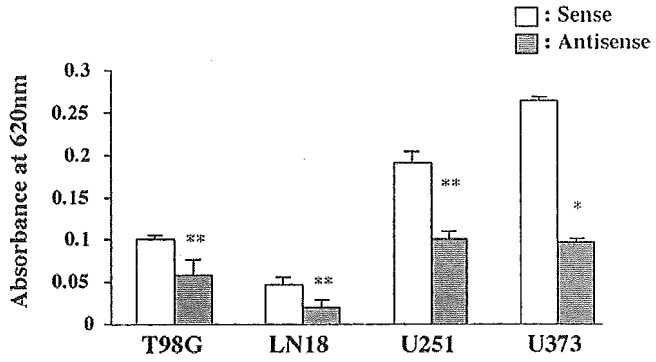

FIGURE 4 – Effects of AS-Ln-α4 on glioma cell adhesion. Glioma cells treated with S-Ln-α4 or AS-Ln-α4 seeded on 96-well culture plates were incubated for 24 hr at 37°C. Adherent cells were stained with toluidine blue, washed with PBS and resolved in 100 µl of 1% SDS. Absorbance was measured at 620 nm using a microplate reader. Values represent means ± SD of 8 experiments. $*p < 0.01$, $**p < 0.0001$ *vs.* sense.

nin β2 chain mRNA was undetectable in T98G, and levels were extremely low in LN18, U251 and U373. These findings suggest that laminin-8 is predominantly expressed compared to laminin-9 or -14 in the 4 glioma cell lines.

Downregulation of laminin α4 chain expression by antisense oligonucleotide

Laminin α4 chain protein levels in conditioned medium after introducing AS-Ln-α4 or S-Ln-α4 were assayed by Western blotting. Although there were some differences in expression of laminin α4 chain among the cell lines, glioma cells treated with S-Ln-α4 clearly expressed α4 chain proteins (Fig. 2*a*). S-Ln-α4

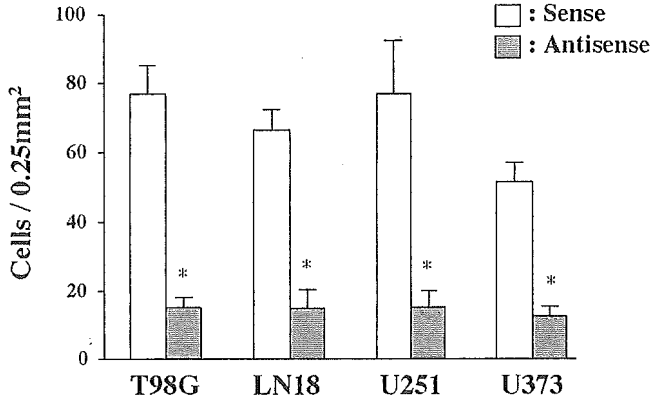

FIGURE 5 – Effects of AS-Ln-α4 on migration activity of glioma cells. Cells that had migrated to the lower surface of the membrane were counted. Cells were incubated with S-Ln-α4 or AS-Ln-α4 immediately before assay. Values represent means ± SD of 8 experiments. $*p < 0.0001$ *vs.* sense.

was therefore used as a control for AS-Ln-α4. To confirm the effective period of AS-Ln-α4 on laminin α4 chain expression, glioma cells transfected with AS-Ln-α4 were cultured for 3, 5 and 7 days. On day 3, laminin α4 proteins were not detected, whereas emergence of the proteins was apparent on days 5 and 7 in all cell lines (Fig. 2*b,c*). As a consequence, we performed subsequent studies on day 3 after the antisense treatment.

In addition, we examined the influence of AS-Ln-α4 or S-Ln-α4 on cell viability and proliferative potential using trypan blue exclusion. Cell growth and viability did not differ between the treatment with AS-Ln-α4 and S-Ln-α4. (Fig. 3).

Decrease of laminin α4 chain suppresses glioma cell adhesion, migration and invasion in vitro

To examine the effects of laminin α4 chain on glioma cell adhesion, cell lines were cultured in serum-free conditioned medium, with cells treated with AS-Ln-α4 or S-Ln-α4 on uncoated plastic plates for 24 hr. Adhesion of cells treated with AS-Ln-α4 was significantly repressed compared to cells treated with S-Ln-α4 (Fig. 4).

We examined the effects of laminin α4 chain on the migratory ability of glioma cells using the modified Boyden chamber method. Conditioned medium of glioma cells containing AS-Ln-α4 or S-Ln-α4 was employed as a chemoattractant in the lower wells of microchemotaxis chambers. Glioma cells treated with S-Ln-α4 migrated to the lower side of the membrane, whereas the migration of those treated with AS-Ln-α4 was suppressed. AS-Ln-α4 significantly inhibited the migration of all glioma cell lines compared to S- Ln-α4 after incubation for 4 hr (Fig. 5).

To investigate whether the downregulation of laminin α4 chain expression impairs cell invasion, we examined the effects of AS-Ln-α4 on glioma cell invasion through collagen IV gel. U373 glioma cells treated with S-Ln-α4 invaded through the collagen IV gel. By contrast, virtually none of the cells treated with AS-Ln-α4 invaded the collagen IV gel (Fig. 6*a*). Invasive cells treated with AS-Ln-α4 or S-Ln-α4 were counted at 1, 2 and 3 days after incubation. After 3 days, the invasive ability of glioma cells transfected with AS-Ln-α4 was significantly reduced compared to cells treated with S-Ln-α4 (Fig. 6*b*).

FIGURE 6 – Effects of AS-Ln-α4 on glioma cell invasion *in vitro*. *(a)* Microphotographs show that U373 glioma cells invaded collagen IV gel to the lower side of the insert filter with 8 µm pores on days 1, 2 and 3. Conditioned medium from U373 glioma cells incubated with S-Ln-α4 or AS-Ln-α4 served as chemoattractant in lower wells of Falcon 24-well plates. Filters were stained with Diff-Quick. Original magnification ×200. Left, S-Ln-α4. Right, AS-Ln-α4. *(b)* Number of invading cells of 4 glioma cell lines with or without antisense treatment counted after 1, 2 and 3 days' incubation. Values represent means ± SD of 8 experiments. $*p < 0.0002$, $**p < 0.0001$ *vs.* sense.

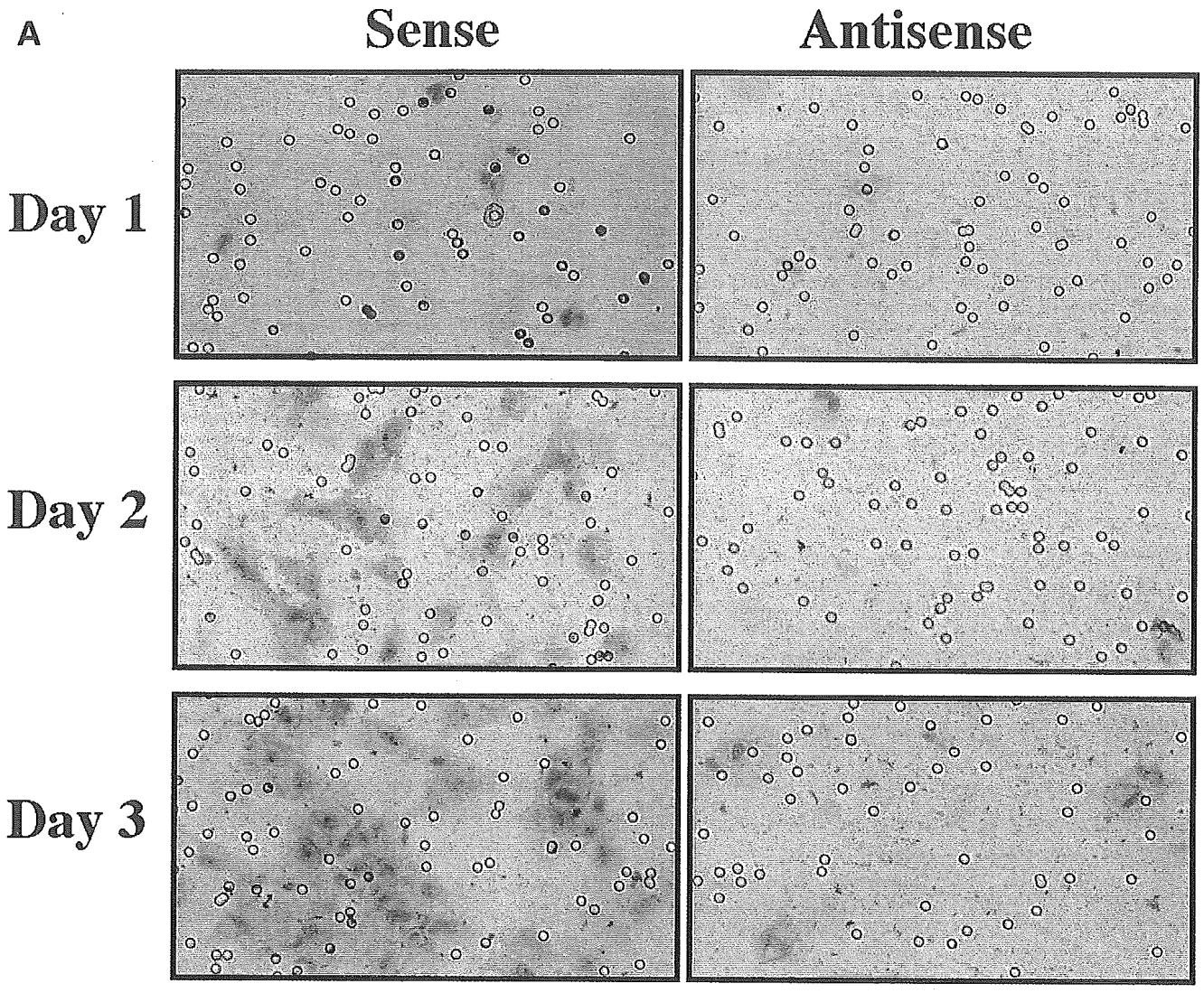
A
Sense
Antisense
Day 1
Day 2
Day 3

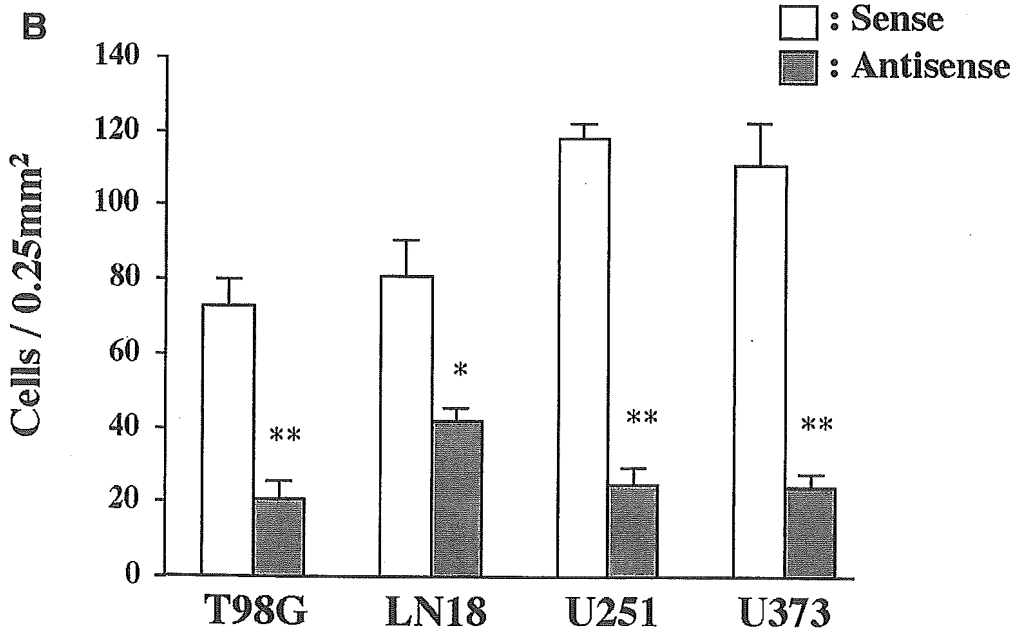
B
: Sense
: Antisense
Cells / 0.25mm²
140
120
100
80
60
40
20
0
**
*
**
**
T98G
LN18
U251
U373

FIGURE 6.

Suppression of α4 chain–containing laminin expression inhibits glioma cell motility in brain slices and an animal model

To evaluate the effects of AS-Ln-α4 on cell motility under more physiologic conditions, we examined how far glioma cells transfected with AS-Ln-α4 or S-Ln-α4 could migrate on organotypic rat brain slices. We implanted rhodamine-labeled spheroids of each glioma cell line in the corpus callosum of the cerebral hemisphere (Fig. 7*a*). Glioma cells treated with S-Ln-α4 actively migrated toward and invaded brain tissues around the tumor spheroids, whereas cells treated with AS-Ln-α4 hardly migrated or invaded beyond the spheroids in any cell line (Fig. 7*b,c*).

To assess the effect of a reduced amount of laminin α4 chain *in vivo,* we transplanted rhodamine-labeled U373 glioma cells that had been transfected with AS-Ln-α4 or S-Ln-α4 into the brains of nude mice. Three days later, whole brains were removed and serially cut into coronal slices. Tumor volume, as assessed by H&E staining, did not differ between the AS-Ln-α4-treated group and the S-Ln-α4-treated group. Fluorescence microscopy revealed that cells harboring S-Ln-α4 invaded diffusely into the brain tissue around the tumor. In contrast, glioma cells treated with AS-Ln-α4 formed noninvasive solid tumors (Fig. 8).

Discussion

In the present series of experiments, downregulated laminin α4 chain expression reduced the motility of human malignant glioma cells both *in vitro* and *in vivo.* Laminin α4 chain is a component of laminin-8 (α4β1γ1) and laminin-9 (α4β2γ1), both of which are overexpressed in some malignant neoplasms.[9,12,13] In one report, high levels of laminin-8 expression were recognized in approximately 75% of glioblastoma cases, whereas laminin-9 was mainly expressed in low-grade gliomas and benign brain tumors. The data also suggest that laminin-8 may contribute to tumor recurrence after therapy of malignant gliomas by facilitating tumor invasion.[15] Therefore, we hypothesized that specific inhibition of laminin-8 might present a novel therapy for high-grade glioma.

We analyzed the expression profiles of α4 chain–containing laminins in human malignant glioma cell lines. PCR data showed that levels of laminin α4 and β1 mRNA were higher than that of laminin β2 chain mRNA in all cell lines tested. This indicates that laminin-8 is synthesized rather than laminin-9 or -14 in glioma cells and that the glioma cell lines used here have the same properties as human malignant gliomas with respect to laminin isoforms.

To investigate the role of laminin α4 chain in glioma cell motility, we assayed cell adhesion, migration and invasion by inhibiting laminin α4 chain with an antisense oligonucleotide. The antisense to laminin α4 chain, which was designed in the present study, completely suppressed expression of the laminin α4 chain protein, proving that AS-Ln-α4 is an extremely effective tool for assessing intracellular events. Migration and invasion were significantly inhibited by downregulation of laminin α4 chain expression.

The biologic significance of α4 chain–containing laminins in invading tumor cells has been obscure. It has been reported that laminin-8 potently promotes cell migration compared to other isoforms of laminin and fibronectin *in vitro.*[18,19,32,33] However, *in vitro* studies alone could not assess glioma invasion because this process is extremely complex and intimately involves the ECM intrinsic to the brain and normal brain architecture. To overcome these problems, we established organotypic brain slice cultures that are analogous to the conditions of the normal brain *in vivo.*[30] The model is nonimmunogenic, and the intrinsic ECM structure is preserved along with the normal brain architecture.[30,34] We there-

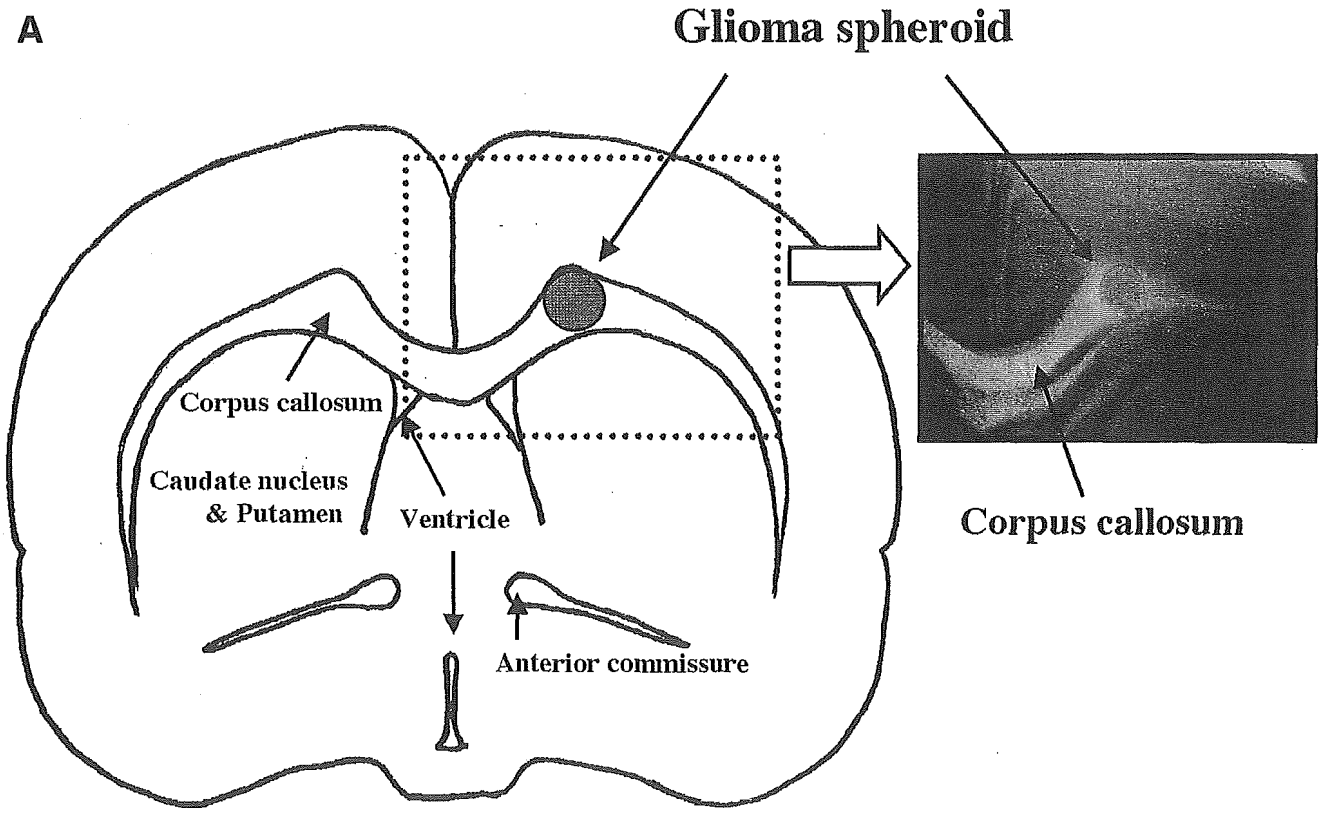

FIGURE 7 – Invasive behavior of glioma cells treated with AS-Ln-α4 on rat brain slices. *(a)* Spheroids (300–400 μm in diameter) of glioma cells labeled with fluorescent PKH26 (rhodamine) were cocultured with rat brain slices (550 μm thick) for 3 days. *(b)* Fluorescent microphotographs with brightfield overlay show the cell invasion of U373 glioma spheroids (arrows) treated with S-Ln-α4 (upper) or AS-Ln-α4 (lower) on a sliced brain tissue. Left, day 0. Right, day 3. Original magnification ×40. *(c)* Fluorescent microphotographs show the cell invasion of T98, LN18 and U251 glioma cells treated with S-Ln-α4 (upper) or AS-Ln-α4 (lower) on day 3.

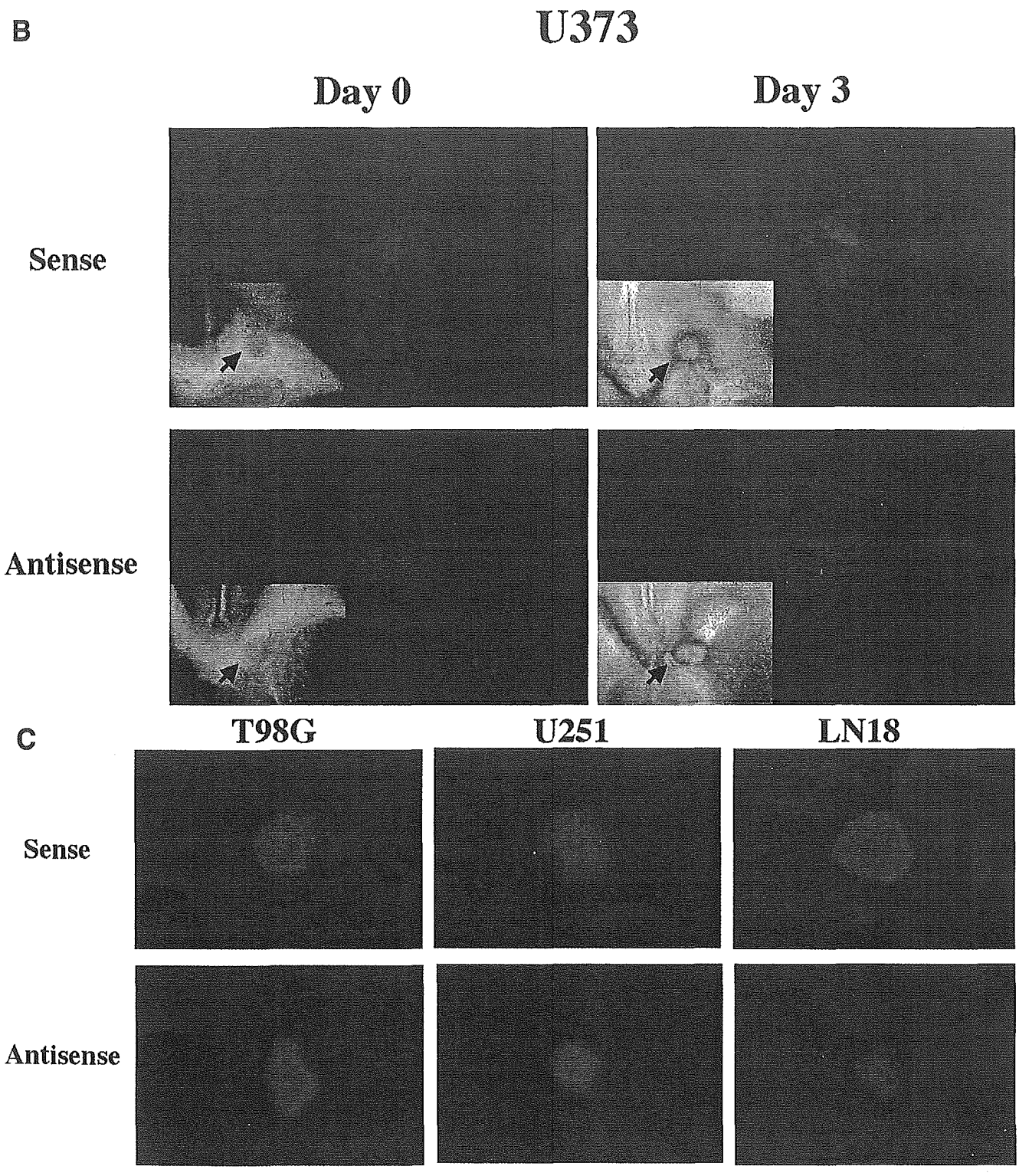

FIGURE 7 – CONTINUED.

fore investigated glioma cell migration and invasion using this model. Cocultures of glioma spheroids and rat brain slices demonstrated that the motility of glioma cells was apparently inhibited by downregulation of laminin α4 chain expression. In addition, our *in vivo* study demonstrated that AS-Ln-α4 prevented U373 glioma cells from developing into invasive brain tumor in nude mice, whereas S-Ln-α4 permitted these cells to form invasive tumor. These findings indicate that an α4 chain–containing laminin, perhaps laminin-8, plays an essential role in glioma cell invasion *in vitro* and *in vivo*.

The ECM creates a dynamic environment with an indispensable function in regulating cell behavior during pathologic remodeling processes such as tumor invasion and metastasis. In contrast to other organ systems, the structure and functions of

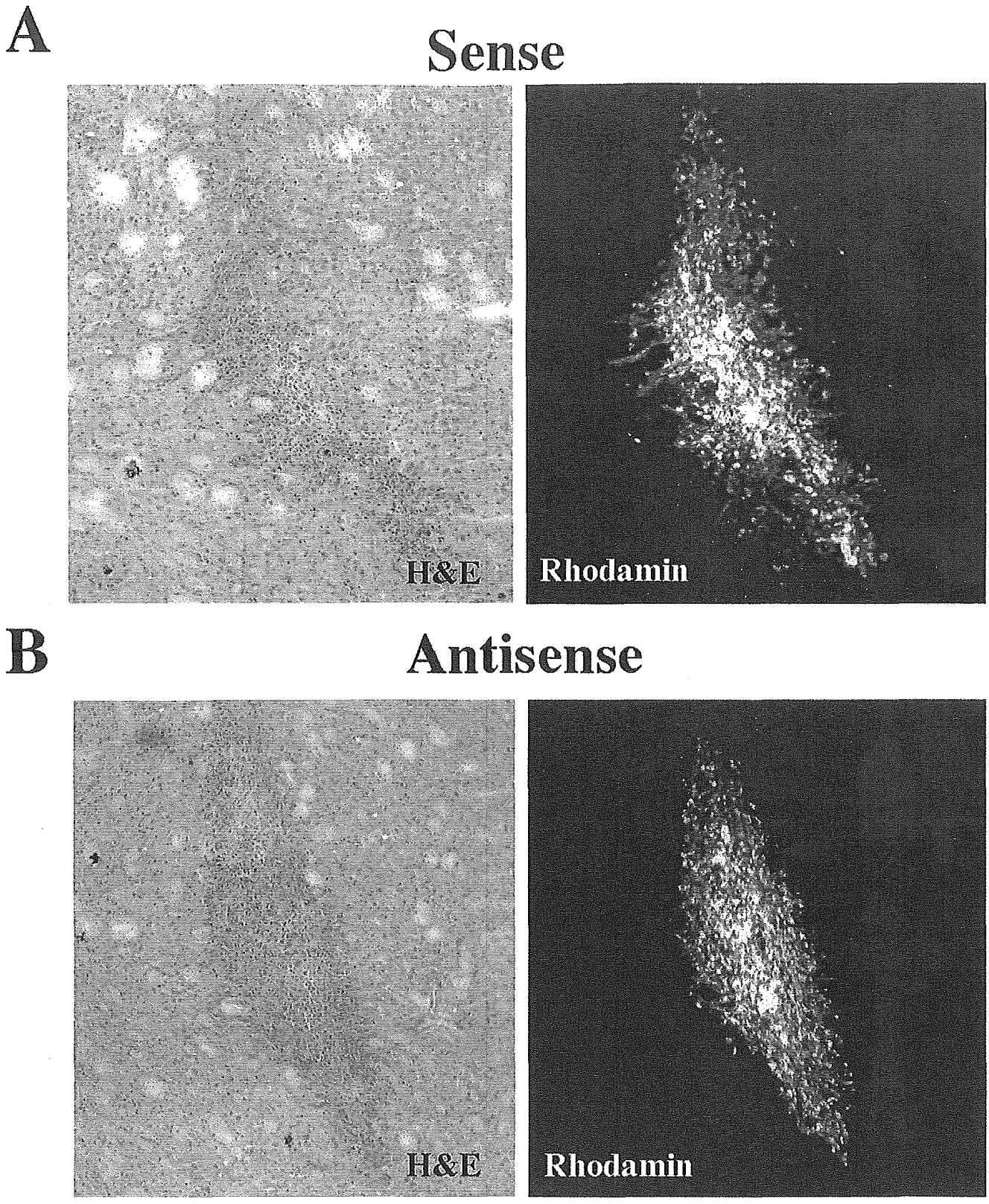

FIGURE 8 – Effects of AS-Ln-α4 on invasive activity of glioma cells transplanted into nude mouse brain. Rhodamine-labeled U373 human glioma cells treated with S-Ln-α4 or AS-Ln-α4 were stereotactically injected into the brains of nude mice. Three days after glioma cell transplantation, cell invasion was observed. *(a)* Microphotographs showing invasive tumor after intracerebral transplantation of S-Ln-α4-treated glioma cells. Left, H&E. Right, fluorescent microphotograph. *(b)* Microphotographs show relatively solid noninvasive tumor mass after intracerebral transplantation of glioma cells treated with AS-Ln-α4. Original magnification ×100.

the ECM in the nervous system remain unknown, and the molecular mechanisms of interaction between glioma cells and the ECM remains unclear. In general, cancer cell motility involves integrin signaling, focal-contact formation and actomyosin-dependent contractility controlled by Rac, Rho or myosin light-chain kinase signaling pathways.[28,35–38] Laminins affect cell functions, including adhesion, migration and differentiation, through binding to integrins. Integrins α6β1 and α3β1 are laminin-8 receptors. One report indicated that Rac was activated during endothelial cell adhesion to laminin-8 and pivotal for α6β1 integrin–mediated cell spreading and migration on laminin-8.[39] Other studies have demonstrated that high levels of β1 integrin subunit are expressed in glioma cells,[31] and stimulation of the β1 integrin subunit increases the activation of MMP-2, which is the most crucial proteinase in the invasiveness of glioma cells.[40–44] We reported that cells migrating from malignant glioma spheroids can be stained with anti-MMP-2 antibody, despite poor staining of the spheroid itself.[30] We have not fully clarified the biologic mechanism through which glioma cell motility is suppressed by the downregulation of laminin α4 chain expression. Further studies are required to elucidate the relation between α4 chain–containing laminins and glioma invasion from the aspect of intracellular signaling events.

In conclusion, the present results show that downregulation of laminin α4 chain using antisense oligonucleotides inhibits the motility of human glioma cells. Laminin α4 chain thus appears to be an important factor in glioma migration and invasion, both *in vitro* and *in vivo*. More detailed understanding of the function and regulation of α4 chain–containing laminin, laminin-8, should ensure the development of effective antiinvasion therapies for patients with malignant glioma.

Acknowledgements

We thank Mr. K. Oka for help in preparing the culture medium.

References

1. Shapiro WR, Shapiro JR. Biology and treatment of malignant glioma. Oncology 1998;12:233–40.
2. Rutka JT, Apodaca G, Stern R, Rosenblum M. The extracellular matrix of the central and peripheral nervous system. J Neurosurg 1988;69:155–70.
3. Bellon G, Caulet T, Cam Y, Pluot M, Poulin G, Pytlinska M, Bernard MH. Immunohistochemical localization of macromolecules of the basement membrane and extracellular matrix of human gliomas and meningiomas. Acta Neuropathol 1985;66:245–52.
4. Carbonetto S. The extracellular matrix of the nervous system. Trends Neurosci 1984;7:382–7.
5. Chintala SK, Sawaya R, Gokaslan ZL. Immunohistochemical localization of extracellular matrix proteins in human glioma, both in vivo and in vitro. Cancer Lett 1996;101:107–14.
6. Kochi N, Tani E, Morimura T, Itagaki T. Immunohistochemical study of fibronectin in human glioma and meningioma. Acta Neuropathol 1983;59:119–26.
7. Mccomb RD, Bigner DD. Immunolocalization of laminin in neoplasms of the central and peripheral nervous systems. J Neuropathol Exp Neurol 1985;44:242–53.
8. Venstrom KA, Reichard LF. Extracellular matrix 2: role of extracellular matrix molecules and their receptors in the nervous system. FASEB J 1993;7:996–1003.
9. Colognato H, Yurchenco PD. Form and function: the laminin family of heterotrimers. Dev Dyn 2000;218:213–34.
10. Friedlander DR, Zagzag D, Shiff B, Cohen H, Allen JC, Kelly PJ, Grumet M. Migration of brain tumor cells on extracellular matrix proteins in vitro correlates with tumor type and grade and involves av and al integrins. Cancer Res 1996;56:1939–47.
11. Giese A, Rief MD, Tran NL, Berens ME. Specific attachment and migration of human astrocytoma cells on human but not murine laminin. Glia 1995;13:64–74.
12. Miner JH, Patton BL, Lentz SI, Gilbert DJ, Snider WD, Jenkins NA, Copeland NG, Sanes JR. The laminin α chains: expression, developmental transitions, and chromosomal locations of α1–5, identification of heterotrimeric laminin8–11, and cloning of a novel α3 isoform. J Cell Biol 1997;137:685–701.
13. Patarroyo M, Tryggvason K, Virtanen I. Laminin isoforms in tumor invasion, angiogenesis and metastasis. Semin Cancer Biol 2002;12:197–207.
14. Ljubimova JY, Lakhter AJ, Loksh A, Yong WH, Riedinger MS, Miner JH, Sorokin LM, Ljubimov AV, Black KL. Overexpression of α4 chain-containing laminins in human glial tumors identified by gene microarray analysis. Cancer Res 2001;61:5601–10.
15. Ljubimova JY, Fugita M, Khazenzon NM, Das A, Pikul BB, Newman D, Sekiguchi K, Sorokin LM, Sasaki T, Black KL. Association between laminin-8 and glial tumor grade, recurrence, and patient survival. Cancer 2004;101:604–12.
16. Gonzales AM, Gonzales M, Herron GS, Nagavarapu U, Hopkinson SB, Tsuruta D, Jones JC. Complex interactions between the laminin α4 subunit and integrins regulate endothelial cell behavior in vitro and angiogenesis in vivo. Proc Natl Acad Sci USA 2002;99:16075–80.
17. Chomczynski P, Sacchi N. Single step method of RNA isolation by acidic guanidinium thiocyanate phenol-chloroform extraction. Anal Biochem 1987;162:156–9.
18. Pedraza C, Geberhiwot T, Ingerpuu S, Assefa D, Wondimu Z, Kortesmaa J, Tryggvason K, Virtanen I, Patarroyo M. Monocytic cells synthesize, adhere to, and migrate on laminin-8 (α4β1γ1). J Immunol 2000;165:5831–8.
19. Fujiwara H, Kikkawa Y, Sanzen N, Sekiguchi K. Purification and characterization of human laminin-8: laminin-8 stimulates cell adhesion and migration through α3β1 and α6β1 integrins. J Biol Chem 2001;276:17550–8.
20. Hathaway WE, Newby LA, Githens JH. The acridine orange viability test applied to bone marrow cells. I. Correlation with trypan blue and eosin dye exclusion and tissue culture transformation. Blood 1964;23:517–25.
21. Murayama O, Nishida H, Sekiguchi K. Novel peptide ligands for integrin α6β1 selected from a phage display library. J Biochem 1996;120:445–51.
22. Ohnishi T, Arita N, Hayakawa T. Motility factor produced by malignant glioma cells: role in tumor invasion. J Neurosurg 1990;73:881–8.
23. Ohnishi T, Arita N, Hiraga S. Fibronectin-mediated cell migration promotes glioma cell invasion through chemokinetic activity. Clin Exp Metastasis 1997;15:538–46.
24. Albini A, Iwamoto Y, Kleinman HK, Martin GR, Aaronson SA, Kozlowski JM, McEwan RN. A rapid in vitro assay for quantitating the invasive potential of tumor cells. Cancer Res 1987;47:3239–45.
25. Amer AP, De Armond SJ, Spencer DR, Coopersmith PF, Ramos DM, Rosenblum ML. Development of an in vitro extracellular matrix assay for studies of brain tumor cell invasion. J Neurooncol 1994;20:1–15.
26. Ohnishi T, Arita N, Hayakawa T, Kawahara K, Kato K, Kakinuma A. Purification of motility factor (GMF) from human malignant glioma cells and its biological significance in tumor invasion. Biochem Biophys Res Commun 1993;193:518–25.
27. Schor SL, Schor AM, Winn B. The use of three-dimensional collagen gels for the study of tumor cell invasion in vitro: experimental parameters influencing cell migration into the gel matrix. Int J Cancer 1982;29:57–62.
28. Somlyo AV, Phelps C, Dipierro C, Eto M, Read P, Barrett M, Gibson JJ, Burnitz MC, Somlyo AP. Rho kinase and matrix metalloproteinase inhibitors cooperate to inhibit angiogenesis and growth of human prostate cancer xenotransplants. FASEB J 2003;17:223–34.
29. Murakami M, Goto S, Yoshikawa M, Goto T, Hamasaki T, Rutka JT, Kuratsu J, Ushio Y. The invasive features of glial and non-central nervous system tumor cells are different on organotypic brain slices from newborn rats. Int J Oncol 2001;18:721–7.
30. Ohnishi T, Matsumura H, Izumoto S, Hiraga S, Hayakawa T. A novel model of glioma cell invasion using organotypic brain slice culture. Cancer Res 1998;58:2935–40.
31. Horan PK, Melnicoff MJ, Jensen BD, Slezak SE. Fluorescent cell labeling for in vivo and in vitro cell tracking. Methods Cell Biol 1990;33:469–90.
32. Hayashi Y, Kim KH, Fujiwara H, Shimono C, Yamashita M, Sanzen N, Futaki S, Sekiguchi K. Identification and recombinant production of human laminin α4 subunit splice variants. Biochem Biophys Res Commun 2000;299:498–504.
33. Kaneko K, Satoh K, Masamune A, Satoh A, Shimosegawa T. Myosin light chain kinase inhibitors can block invasion and adhesion of human pancreatic cancer cell lines. Pancreas 2002;24:34–41.
34. Stoppini L, Buchs PA, Muller D. A simple method for organotypic cultures of nervous tissue. J Neurosci Methods 1991;37:173–82.

35. Friedl P, Zanker KS, Bröcker EB. Cell migration strategies in 3-D extracellular matrix: differences in morphology, cell matrix interactions, and integrin function. Microsc Res Tech 1998;43:369–78.
36. Itoh K, Yoshioka K, Akedo H, Uehata M, Ishizaki T, Narumiya S. An essential part for Rho-associated kinase in the transcellular invasion of tumor cells. Nat Med 1999;5:221–5.
37. Khazenzon NM, Ljubimov AV, Lakhter AJ, Fujita M, Fujiwara H, Sekiguchi K. Antisense inhibition of laminin-8 expression reduces invasion of human gliomas in vitro. Mol Cancer Ther 2003;2:985–94.
38. Yoshioka K, Nakamori S, Itoh K. Overexpression of small GTP-binding protein RhoA promotes invasion of tumor cells. Cancer Res 1999;59:2004–10.
39. Fujiwara H, Gu J, Sekiguchi K. Rac regulates integrin-mediated endothelial cell adhesion and migration on laminin-8. Exp Cell Res 2004;292:67–77.
40. Deryugina EI, Bourdon MA, Reisfeld RA, Strongin A. Remodeling of collagen matrix by human tumor cells requires activation and cell surface association of matrix metalloproteinase-2. Cancer Res 1998;58:3743–50.
41. Nabeshima K, Inoue T, Shimao Y, Okada Y, Itoh Y, Seiki M, Koono M. Front-cell-specific expression of membrane-type 1 matrix metalloproteinase and gelatinase A during cohort migration of colon carcinoma cells induced by hepatocyte growth factor/scatter factor. Cancer Res 2000;60:3364–9.
42. Ohuchi E, Imai K, Fujii Y, Sato H, Seiki M, Okada Y. Membrane type 1 matrix metalloproteinase digests interstitial collagens and other extracellular matrix macromolecules. J Biol Chem 1997;272:2446–51.
43. Sawaya RE, Yamamoto M, Gokaslan ZL. Expression and localization of 72 kDa type IV collagenase (MMP-2) in human malignant gliomas in vivo. Clin Exp Metastasis 1996;14:35–42.
44. Uhm JH, Dooley NP, Villemure JG, Yong VW. Glioma invasion in vitro: regulation by matrix metalloprotease-2 and protein kinase C. Clin Exp Metastasis 1996;14:421–33.

III. 脳腫瘍の病理

脳腫瘍の分類
概　論

Classification of brain tumors: introduction

大西丘倫

Key words　脳腫瘍分類，WHO分類，脳腫瘍病理

1. 脳腫瘍分類の歴史

脳腫瘍は他の臓器の腫瘍と比べ，発生母地の異なる極めて多種の腫瘍型を含んでおり，1979年に世界的に統一された組織分類が集大成されるまで様々な分類法が行われてきた．そのような脳腫瘍の組織分類の歴史の中で，2つの特筆すべき分類がある．一つは，形態学的類似性から腫瘍の発生母細胞を想定して命名するという組織発生学的分類を行ったBailey and Cushingの分類(1926年)であり，他の一つは，脳腫瘍組織と臨床的予後との関係を'grading'という指標で示したKernohan and Sayreの分類(1952年)である．

BaileyとCushingは，中枢神経系の組織発生あるいは細胞発生の過程に出現する各段階の未分化細胞と神経外胚葉由来の腫瘍の組織細胞所見とを照らし合わせ，形態学的アナロジーにより腫瘍を分類した(**図1**)[1]．すなわち，胎生初期の髄上皮(medullary epithelium)から発生してくる20種類の細胞を分類し，それらの細胞形態に対応させて各腫瘍の発生起源を類推し，その形態を基に16種類の腫瘍を命名している．その中にはglioblastoma multiformeやmedulloblastomaなど，現在なお使用されている腫瘍名が多く存在している．彼らの分類は単に腫瘍組織を初めて系統的に分類しただけでなく，腫瘍組織と悪性度を関連づけ，常に臨床的意義を意識した分類であり，今日の脳腫瘍分類の基礎を築いたといっても過言ではない．

その後，臨床的な必要性から腫瘍の悪性度に応じた分類が試みられ，KernohanとSayreは，グリオーマを組織学的悪性度に対応させ，grade 1(良性)からgrade 4(最悪性)までの4段階に分類した(**表1**)[2]．この分類法はわかりやすく臨床的にも広く普及したが，星細胞系腫瘍以外はgradingを4つに分ける意義が明確でなく実際にはほとんど用いられなかった．ちなみにKernohanは，この分類でglioblastoma multiformeの名称を用いずにastrocytoma grade 4の名称を用いている．同様なgradingをRingertz[3]も発表しているが，Kernohanとは異なり3段階のgradeに分類している．Ringertzは，oligodendrogliomaやependymomaが悪性化していく過程でglioblastomaに転化する例があることを示し，その後の腫瘍病態に重要な示唆を与えた．ただこれらのgradingによる分類は，臨床的に必ずしも予後を反映せず，また，名称が病理学者間で一致しないこともあり，満足のいく分類法とはならなかった．

Takanori Ohnishi: Department of Neurosurgery, Ehime University School of Medicine　愛媛大学医学部 脳神経外科

0047-1852/05/¥40/頁/JCLS

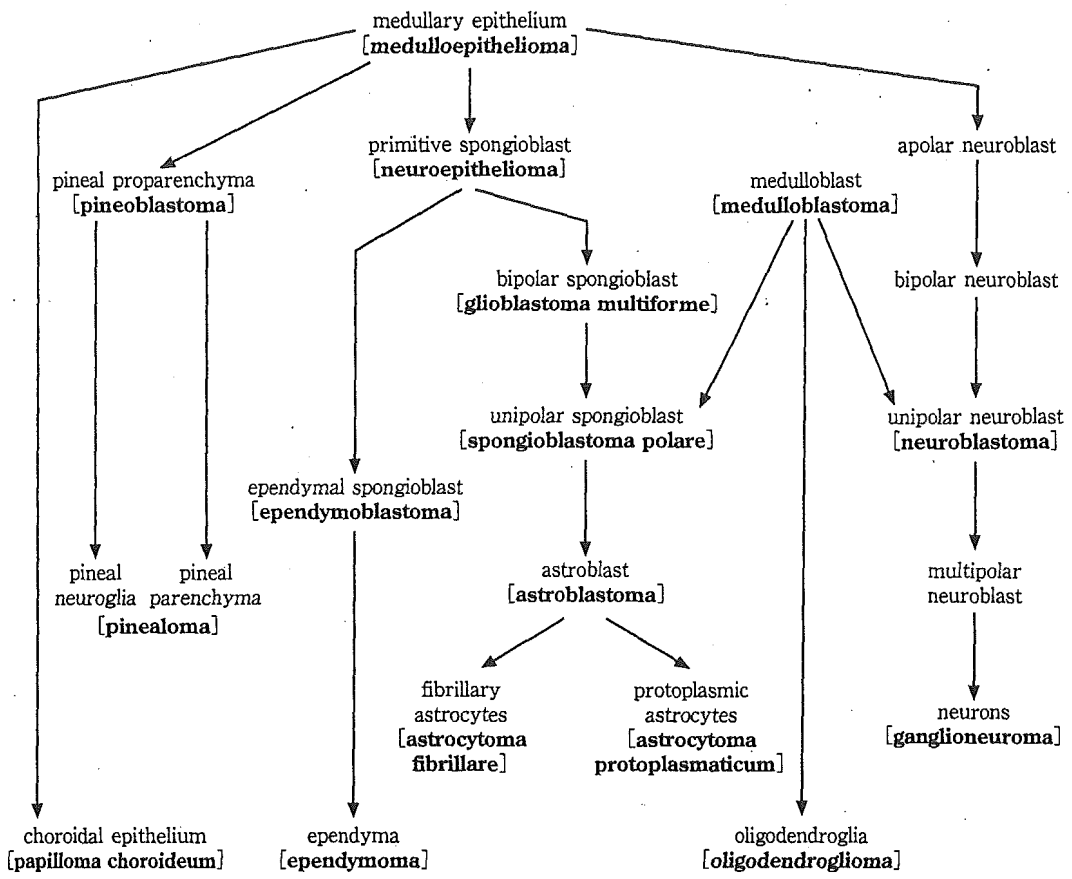

図1 Bailey-Cushing分類
中枢神経系組織の発生(上段)と形態学的に対比した腫瘍分類(下段).

2. WHO分類

20世紀半ば過ぎからの脳腫瘍研究の急速な進展に伴い，多くの研究者が独自の分類法を発表するようになった．その結果，同一腫瘍名でも全く異なった種類の腫瘍を表すという混乱が生じた．そこで，脳腫瘍の分類を国際的に統一すべく，WHOに設置された腫瘍の国際分類に関する委員会の分科会として，脳腫瘍組織学的分類の委員会が1970年に発足した．その成果は1979年，'Histological Typing of Tumours of the Central Nervous System'(いわゆるWHO分類)として刊行された[4]．この分類では，従来よく用いられていた名称は尊重しながらも腫瘍名を統一する努力が払われ，また臨床的悪性度を示す指標として4段階で分けられたWHO grading を採用していることが特徴の一つである．その後，免疫組織化学や電子顕微鏡を駆使した腫瘍の組織学的診断法の進歩により，primitive neuroectodermal tumor(PNET)などの新しい腫瘍型が次々と提唱され，旧分類では対応できなくなったことから，1993年にWHO分類第2版として改訂された[5]．この改訂版の特徴は，可能なかぎり組織発生に基づいて分類し，組織発生が不明な腫瘍を別にしたことと，それまで別扱いされていたglioblastoma multiformeがastrocytic tumors(星細胞系腫瘍)の中に分類されたことなどである．後者については，両者の間でGFAPの発現などの免疫組織学的特徴やp53遺伝子異常などの分子生物学的特徴が共通していることが加味された結果であろう．

このように形態学を中心とした脳腫瘍組織分